Food and Chemical Toxicology 65 (2014) 33–42

Contents lists available at ScienceDirect

Food and Chemical Toxicology

journal homepage: www.elsevier.com/locate/foodchemtox

The ethanol extract of *Zingiber zerumbet* Smith attenuates non-alcoholic fatty liver disease in hamsters fed on high-fat diet

Chia Ju Chang, Shorong-Shii Liou, Thing-Fong Tzeng, I-Min Liu *

Department of Pharmacy & Graduate Institute of Pharmaceutical Technology, Tajen University, Yanpu Shiang, Ping Tung Shien, Taiwan, ROC

ARTICLE INFO

Article history:
Received 10 August 2013
Accepted 29 November 2013
Available online 14 December 2013

Keywords:
High-fat diet
Non-alcoholic fatty liver disease
Peroxisome proliferator-activated receptor α
Sterol regulatory element-binding protein-1c
Zingiber zerumbet rhizome

ABSTRACT

The beneficial effects of the ethanol extract of *Zingiber zerumbet* rhizome (EEZZR) for use in the treatment of non-alcoholic fatty liver disease (NAFLD) were investigated. Syrian golden hamsters were fed a high-fat diet to induce NAFLD. EEZZR (100, 200, or 300 mg/kg) were orally administered by gavage once daily for 8 weeks. The higher plasma levels of total cholesterol, triglycerides, free fatty acids, and hepatic lipids, as well as the degree of insulin resistance were lowered by EEZZR. Histological evaluation of liver specimens demonstrated that the hepatic steatosis of EEZZR-treated groups was improved. EEZZR decreased hepatic mRNA levels of sterol regulatory element-binding protein-1c and its lipogenic target genes. The hepatic mRNA expression of peroxisome proliferator-activated receptor α, together with its target genes responsible for β-oxidation of fatty acids were also upregulated by EEZZR. In conclusion, these findings suggest that EEZZR has the promising potential to ameliorate NAFLD.

1. Introduction

Non-alcoholic fatty liver disease (NAFLD) is a potentially severe condition that comprises a spectrum of pathologies characterized by vesicular fatty change in the liver in the absence of excessive alcohol consumption (Ibrahim et al., 2013). NAFLD is strongly associated with obesity, insulin resistance, and type 2 diabetes and is now well recognized as being part of the metabolic syndrome (Paschos and Paletas, 2009). The metabolic pathways leading to the development of hepatic steatosis are multiple, including enhanced non-esterified fatty acid release from adipose tissue (lipolysis), increased *de novo* fatty acids (lipogenesis), and decreased β-oxidation. To date, caloric restriction and aerobic exercise are effective treatments for NAFLD, but they are difficult to achieve for most NAFLD patients. Other than lifestyle and diet modifications, there is no universally proven treatment (Beaton, 2012). Therefore, the development of additional therapies for controlling lipid levels is warranted to attenuate hepatic steatosis.

Zingiber zerumbet, locally known as lempoyang or wild ginger, has been shown to possess a number of biological activities, including anti-cancer, anti-inflammatory, antimicrobial, and antioxidant properties (Yob et al., 2011). *Z. zerumbet* has been shown to contain flavonoid compounds that exhibit antioxidant properties (Yob et al., 2011), and ethyl acetate extract of the plant has been shown to exhibit strong antioxidant activity (Ruslay et al., 2007). Zerumbone, an active component of the *Z. zerumbet* rhizome (ZZR), has been shown to protect against cisplatin-induced renal dysfunction by preventing lipid peroxidation and preserving antioxidant activity (Ibrahim et al., 2010). The ethanol extract of ZZR (EEZZR) resulted in apparent improvement in overall insulin sensitivity by ameliorating hyperinsulinemia and gluconeogenesis (Chang et al., 2012a) and might reduce the accumulation of visceral fat and improve hyperlipidemia in high-fat diet (HFD)-induced rats (Chang et al., 2012b). However, the effects of EEZZR on hepatic hyperlipidemia and the potential mechanism of its effects on lipid metabolism remains unclear.

The effects of dietary cholesterol and fat on plasma lipid profiles are similar in hamsters and humans, and fatty liver and mild diabetes developed in hamsters after being fed a HFD (Bhathena et al., 2011). Hamsters fed a HFD may thus be a good animal model for research on the treatment of diet-induced metabolic syndrome complicated by NAFLD (Bhathena et al., 2011). The aim of this work is to assess the effects of EEZZR on hepatic lipid accumulation in HFD-induced NAFLD hamsters.

2. Materials and methods

2.1. Plant material and extraction

ZZR were purchased from a local market in Dongshan, Dongshan Dist. (Tainan City, Taiwan) during October 2010. Macroscopic and microscopic examinations, thin-layer chromatography, and high-performance liquid chromatography were used to confirm the authenticity of the plant material provided (this analysis was performed by Dr. Hong T.Y., Department of Biotechnology, Collage of Pharmacy and Health Care, Tajen University). Random amplified polymorphic DNA analysis of the ZZR supplied was also performed to identify DNA polymorphisms. The voucher specimen (Lot No. 20101018) has been deposited in our laboratory. For extraction, the plant materials were macerated, air dried, and 3 kg of pulverized ZZR was added to 10 l of 95% ethanol and allowed to stand at room temperature for 7 days

* Corresponding author. Tel.: +886 8 7624002; fax: +886 8 7625308.
E-mail address: iml@tajen.edu.tw (I-Min Liu).

0278-6915/$ - see front matter © 2013 Elsevier Ltd. All rights reserved.
http://dx.doi.org/10.1016/j.fct.2013.11.048

with occasional shaking. EEZZR was evaporated to dryness under reduced pressure for the total elimination of alcohol, followed by lyophilization, yielding approximately 354 g of dry residue (w/w yield: 11.8%). EEZZR was stored at −20 °C until use and suspended in distilled water.

2.2. LC/MS/MS system

Chromatographic separation of the extracts was performed using an HPLC apparatus equipped with two micropumps (Series 200; PerkinElmer, Shellton, CT, USA), a UV/VIS detector (Series 200; PerkinElmer, Shellton, CT, USA) at a wavelength of 280 nm, and a Prodigy ODS3 100A column (250 mm × 4.6 mm; particle size, 5 μm) (Phenomenex, CA, USA). The eluents were (A) 0.2% formic acid in water, and (B) acetonitrile/methanol (60:40, v/v). The following gradient program was used: 20–30% B (6 min), 30–40% B (10 min), 40–50% B (8 min), 50–90% B (8 min), 90–90% B (3 min), 90–20% B (3 min) at a constant flow rate of 0.8 ml/min. The LC flow was split, and 0.2 ml/min was sent to the mass spectrometer. Three 20 μl injections were performed for each sample. MS and MS/MS analyses of EEZZR were performed on an API 4000 triple quadrupole mass spectrometer (Applied Biosystems, Canada) equipped with a Turbolon Spray source and working in the negative ion mode. The analyses were performed using the following settings: drying gas (air), 400 °C; capillary voltage (IS), 4000 V; nebulizer gas (air), 12 (arbitrary units); curtain gas (N_2), 14 (arbitrary units); and collision gas (N_2), 4 (arbitrary units). To optimize the declustering potential, focus potential, and collision energy for each compound, standard solutions (10 μg/ml) were infused directly into the mass spectrometer at a constant flow rate of 5 μl/min using a model 11 syringe pump (Harvard Apparatus, Holliston, MA, USA). Zerumbone (purity ⩾ 98.0%; Sigma–Aldrich, Inc., Saint Louis, Missouri, USA; Cat. # Z3902) kaempferol (purity ⩾ 97.0%; Sigma–Aldrich, Inc.; Cat. # 60010), quercetin (purity ⩾ 98.0%; Sigma–Aldrich, Inc.; Cat. # Q4951) or [6]-gingerol (purity ⩾ 98.0%; Sigma–Aldrich, Inc.; Cat. # G1046) at concentrations of 12.5 to 400 μg/ml were used to construct the standard curve. The retention times of the main compounds were 8.47, 7.19, 6.98, and 7.55 min for zerumbone, kaempferol, quercetin, and [6]-gingerol, respectively. The linearity of the peak area (y) vs. concentration (x, μg/ml) curves for zerumbone, kaempferol, quercetin, and [6]-gingerol were used to calculate the contents of the main components in EEZZR. The standard curves for zerumbone, kaempferol, quercetin, and [6]-gingerol are $y = 46908x + 265257$ ($R^2 = 0.9912$), $y = 297.53x - 333.59$ ($R^2 = 0.9958$), $y = 996.94x - 1.84$ ($R^2 = 0.9969$), and $y = 94432x + 21688$ ($R^2 = 0.9973$), respectively.

2.3. Animal models

Male Golden Syrian hamsters, 8 weeks old and weighing 90 ± 10 g, were obtained from the National Laboratory Animal Center (Taipei, Taiwan). They were maintained in a temperature-controlled room (25 ± 1 °C) on a 12 h:12 h light–dark cycle (lights on at 06:00 h) in our animal center. Food and water were provided *ad libitum*. Regular rat chow diet (RCD, #D12450B, Research Diets, New Brunswick, NJ) with 20 kcal% protein, 70 kcal% carbohydrate, and 10 kcal% fat from lard was used as the maintenance and control diet. A purified ingredient HFD with 20 kcal% protein, 35 kcal% carbohydrate, and 45 kcal% fat primarily from lard (#D12451, Research Diets) was used to induce a rapid increase in body weight and obesity (Van Heek et al., 1997). All animal procedures were performed according to the Guide for the Care and Use of Laboratory Animals of the National Institutes of Health, as well as the guidelines of the Animal Welfare Act. These studies were conducted with the approval of the Institutional Animal Care and Use Committee (IACUC) at Tajen University (approval number, IACUC 100-29; approval date, December 22, 2011).

2.4. Treatment protocols

After being fed a HFD for two weeks, hamsters were dosed by oral gavage once per day for eight weeks with EEZZR doses of 100, 200, and 300 mg/kg in a volume of 1.5 ml/kg distilled water. The selected dosage regime for the present studies was based on a previous report that demonstrated EEZZR at doses of 200 and 300 mg/kg once daily for eight weeks has an ameliorating effect on dyslipidemia in HFD-fed rats (Chang et al., 2012b). Another group of HFD-fed hamsters was treated orally for eight weeks with 100 mg/kg/day lipanthyl (Laboratories Fournier SA, France). Lipanthyl, a fibric acid derivative, is a commercially available drug in the treatment of hyperlipidemia and are generally effective in lowering elevated plasma triglycerides (TG) and cholesterol levels (Kraja et al., 2010). Lipanthyl is thus used to compare the efficacy of EEZZR. The dose of lipanthyl was based on a study reporting that long term lipanthyl treatment could ameliorate hepatic insulin resistance and steatosis in high-fructose-fed mice (Chan et al., 2013). The control groups received water by gavage instead of EZZR. The water consumption, food intake, and body weight were measured once daily at the same time (09:00) on each day throughout the experiment. Food cups containing fresh food were weighed at the beginning and end of each 24-h period. Food intake was calculated by determining the difference in food cup weights, adjusting for any spillage that occurred. Water intake was calculated by measuring the difference in water bottle weights at the beginning and end of the daily change of water.

Eight weeks after treatment with EEZZR (total diet-fed period was 10 weeks), animals were weighed and anesthetized with ketamine after fasting for 12 h. Blood samples were taken from the inferior vena cava for analysis. After blood collection, the liver was removed, rinsed with a physiological saline solution, and immediately stored at −70 °C. The coefficient of hepatic weight was also calculated as liver weight (g) divided by body weight (100 g).

2.5. Determination of metabolic parameters and insulin sensitivity

Blood samples were centrifuged at 2000g for 10 min at 4 °C. The plasma was then removed and placed into aliquots for the respective analyses. Kits for determining plasma glucose (Cat. No. 10009582) concentration was purchased from Cayman Chemical Company (Ann Arbor, MI). Commercial enzyme-linked immunosorbent assay (ELISA) kits were used to quantify plasma insulin concentration (Linco Research, Inc., St. Charles, MO; Cat. #EZRMI-13K). Diagnostic kits for determination of plasma levels of total cholesterol (TC; Cat. # 10007640) and triglycerides (TG; Cat. # 10010303) were purchased from Cayman Chemical Company (Ann Arbor, Michigan, USA). The diagnostic kit for determination of plasma levels of high density lipoprotein cholesterol (HDL-C) was purchased from Bio-Quant Diagnostics (Cat. # BQ 019CR; San Diego, CA, USA). Low density lipoprotein cholesterol (LDL-C) concentrations in plasma were determined by commercial ELISA kit (antibodies-online Inc., Atlanta, GA 30338, USA.; Cat. # ABIN416222). Plasma free fatty acid (FFA) levels were determined using an FFA quantification kit obtained from Abcam plc (Cat. # ab65341; Cambridge, MA, USA). Plasma monocyte chemoattractant protein (MCP)-1 (Cat. # MJE00), tumor necrosis factor (TNF)-α (Cat. # MTA00B) and interleukin (IL)-6 (Cat. # M6000B) were measured using commercial ELISA kits purchased from R&D Systems, Inc. (Minneapolis, MN, USA). All experimental assays were carried out according to the manufacturer's instruction. All samples were analyzed in triplicate.

Whole-body insulin sensitivity was estimated using the homeostasis model assessment of insulin resistance (HOMA-IR) with the following formula: [fasting plasma glucose (mmol) × fasting plasma insulin (mU/ml)]/22.5 (Matthews et al., 1985). Because HOMA is negatively correlated with insulin sensitivity, low HOMA-IR values indicate high insulin sensitivity, whereas high HOMA-IR values indicate insulin resistance.

2.6. Measurement of hepatic lipids

Sections of fresh liver samples were collected for determining the lipid content. Liver (1.25 g) was homogenized with chloroform/methanol (1:2, 3.75 ml). Chloroform (1.25 ml) and distilled water (1.25 ml) were then added to the homogenate and mixed well. After centrifugation (1500g for 10 min), the lower clear organic phase of the solution was transferred into a new glass tube and then lyophilized. The lyophilized powder was dissolved in chloroform/methanol (1:2) and stored at −20 °C for less than 3 days (Folch et al., 1957). Hepatic TC and TG levels in lipid extracts were analyzed using the same diagnostic kits that were used for plasma analysis.

2.7. Histological analysis of the liver

At sacrifice, livers were perfused with phosphate buffered saline (PBS) solution via the portal vein. After removal of the liver, a section of approximately 4 mm^2 was fixed in PAF and embedded in paraffin. Paraffin-embedded sections (5 μm) were stained with hematoxylin and eosin (H&E) to evaluate the degree of hepatic steatosis. Other frozen liver sections were stained with rat monoclonal anti-macrophage F4/80 (1:500, Cat. # sc-377009; Santa Cruz Biotechnology, Santa Cruz, CA, United States), or mouse monoclonal anti-smooth muscle actin (SMA) antibody (1: 500; Santa Cruz Biotechnology) followed by detection with biotinylated secondary antibody and streptavidin-horseradish peroxidase to evaluate the degree of macrophage infiltration and fibrosis. All slides were scanned at a total magnification of 200 × using Image Pro Plus 7.0 software (Media Cybernetics) under a light microscope (Olympus BX51 microscope; Tokyo, Japan).

2.8. Analysis of mRNA expression of hepatic genes

For analysis of gene expression, total RNA was extracted from 100 mg frozen liver samples using Trizol reagent (Invitrogen, USA). RNA was quantified by A260 and its integrity verified by agarose gel electrophoresis using ethidium bromide for visualization. For the reverse transcriptase reaction, 1 μg of total RNA per sample and 8.5 μg/μl random hexamer primers were heated at 65 °C for 5 min and then quenched on ice. This mixture was combined with 500 μmol/l each of dATP, dTTP, dCTP, and dGTP, 10 mmol/l DTT, 20 mmol/l Tris–HCl (pH 8.4), 50 mmol/l KCl, 5 mmol/l $MgCl_2$, 40 units of RNaseOUT™ recombinant ribonuclease inhibitor (Invitrogen; Boston, MA, USA) and 100 units SuperScript III reverse transcriptase (Invitrogen). Samples were subjected to DNase (Promega; Madison, WI, USA) treatment at 37 °C for 20 min in a GeneAmp 9700 Thermal Cycler (Applied Biosystems; Foster City, California, USA) and then held at 4 °C. After aliquots were taken for immediate use in PCR, the remainder of the cDNA was stored at −20 °C. mRNA expression was measured by quantitative real-time RT-PCR in a fluorescent

temperature Lightcycler 480 (Roche Diagnostics; Mannheim, Germany). The sterol regulatory element-binding protein-1c (SREBP-1c) primer sequences were as follows: forward, 5′-CGCTACCGTTCCTCTATCAA-3′; reverse, 5′-TTCGCAGGGTCAGGTTCTC-3′. The acetyl-CoA carboxylase 1 (ACC1) primers were as follows: forward, 5′-GGACAGAC1GATCGCAGAGAAAG-3′; reverse, 5′-TGGAGAGCCCCACACACA-3′. The fatty acid synthase (FAS) primers were as follows: forward, 5′-GGAACTGA ACGGCATTACTCG-3′; reverse, 5′-CATGCCGTTATCAACTTGTCC-3′. The stearoyl-CoA desaturase (SCD)1 primers were as follows: forward, 5′-CCTTAACCCTGAGATCCCGTAGA-3′; reverse, 5′-AGCCCATAAAAGATTTC1GCAAA-3′. The peroxisome proliferator-activated receptor (PPAR) α primers sequences were as follows: forward, 5′-GAAGCAGATGACCTGGAAAGT-3′; reverse, 5′-AGCCTGGACAGCTCCCTAA-3′. The carnitine palmitoyl transferase (CPT)-1 primers sequences were as follows: forward, 5′-GCTTCCCCTTACTGGTTCC-3′; reverse, 5′-AACTGGCAGGCAATGAGACT-3′. The acyl-CoA oxidase (ACO) primers sequences were as follows: forward, 5′-ACTATATTTGGCCAATTTTGTG-3′; reverse, 5′- TGTGGCAGTGGTTTCCAAGCC-3′. The acyl-CoA oxidase 1 (ACOX1) primers sequences were as follows: forward, 5′-GTTGATCACGCACATCTTGGA-3′; reverse, 5′-TCGTTCAGAATCAAGTTCTCAATTTC-3′. The β-actin primers sequences were as follows: forward, 5′-TCACCCACACTGTGCCCATCTA-3′; reverse, 5′-TTGCTGATCCACATCTGCTGG-3′. Primers were designed using Primer Express Software version 2.0 System (Applied Biosystems; Foster City, CA, USA). The PCR reaction was performed using the following cycling protocol: 95 °C for 5 min, followed by 45 cycles of 95 °C for 5 s, 58 °C for 15 s, and 72 °C for 20 s. Dissociation curves were run after amplification to identify the specific PCR products. The mRNA expression levels were normalized to β-actin mRNA levels and calculated according to the delta-delta Ct method (Livak and Schmittgen, 2001).

2.9. Statistical analysis

Data are expressed as the mean ± standard deviation (SD). Statistical analysis was performed with one-way analysis of variance (ANOVA). Dunnett range post hoc comparisons were used to determine the source of significant differences, where appropriate. A p-value < 0.05 was considered statistically significant. For the histological study, a non-parametric Kruskal–Wallis test was performed and Mann–Whitney's U test was used to compare data within the groups. The SigmaPlot (Version 11.0) programme was used for statistical analysis.

3. Results

3.1. Phytochemical analysis

Chemical analysis with LC/MS/MS revealed that EEZZR contained zerumbone (196.24 ± 0.31 μg/g, Fig. 1A). Contents of kaempferol and quercetin in EEZZR were 92.71 ± 0.29 and 86.43 ± 0.24 μg/g, respectively (Fig. 1B and C). The result also showed that EEZZR had a [6]-gingerol content of 100.45 ± 0.31 μg/g (Fig. 1D).

3.2. Effects of treatments on the body weight, the relative liver weights and feeding behaviors of hamsters

At the end of 8 weeks of treatment, the body weight and relative liver weights in HFD-fed hamsters were significantly higher those in the RCD-fed group (Table 1). High doses of EEZZR (300 mg/kg/day) significantly suppressed body weight gain. The coefficient of hepatic weight in EEZZR (300 mg/kg/day)-treated HFD-fed hamsters was significantly lower than that of the vehicle-treated group. Similar results were seen in HFD-fed hamsters treated with lipanthyl (100 mg/kg/day) (Table 1). No significant differences in daily food or water intake were observed between the groups over the experimental period (Table 1).

3.3. Effects of treatments on insulin sensitivity and plasma lipids levels of hamsters

HFD-fed hamsters were insulin resistant as reflected by hyperinsulinemia as well as significantly increased HOMA-IR values (Table 1). Treatment of HFD-fed hamsters with EEZZR (300 mg/kg/day) had an effect on insulin resistance similar to that of lipanthyl, as evidenced by a reduction in fasting serum insulin levels and improved levels of HOMA-IR (Table 1).

The HFD caused elevated concentrations of plasma TC, TG, and LDL-C. EEZZR at the oral dose of 200 or 300 mg/kg/day significantly reduced total plasma TC levels (13.1% and 17.3% reduction, respectively) compared to that of vehicle-treated HFD-fed hamsters (Table 1). All doses of EEZZR decreased plasma TG levels in HFD-fed hamsters; the reduction of plasma TG activity induced by EEZZR at 300 mg/kg/day was nearly 35.2% (Table 1). Oral administration of EEZZR at a dose of 100, 200, or 300 mg/kg/day significantly reduced plasma LDL-C levels (6.7%, 16.8%, and 22.2% reduction, respectively) (Table 1). Plasma TC, TG, and LDL-C concentrations were significantly reduced in lipanthyl-treated HFD-fed hamsters compared with their vehicle-treated counterparts by 20.7%, 48.9%, and 27.8%, respectively (Table 1).

The plasma concentration of HDL-C in HFD-fed hamsters was reduced to 71.3% of the level observed in the RCD-fed group (Table 1). After 8 weeks of treatment with EEZZR

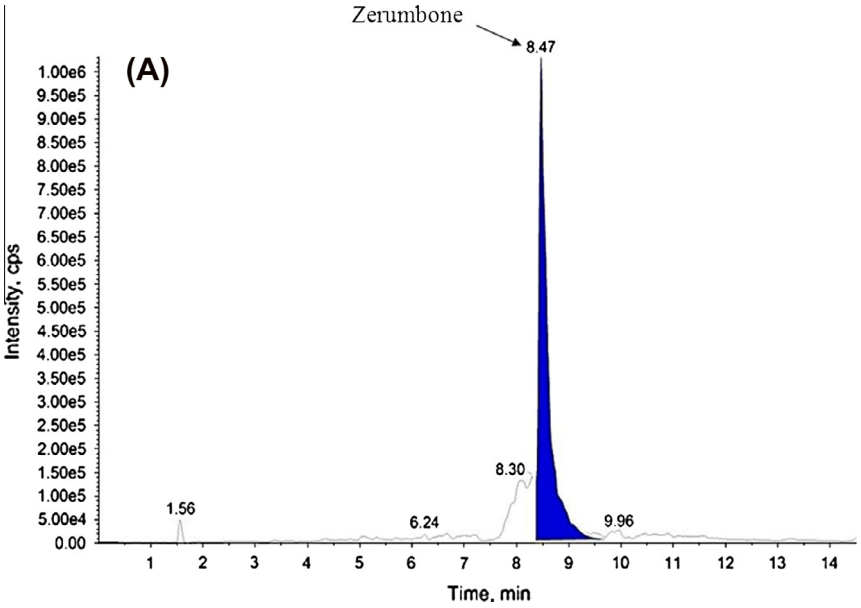

Fig. 1. LC/MS/MS chromatograms of zerumbone (A), kaempferol (B), quercetin (C), and [6]-gingerol (D) in EEZZR.

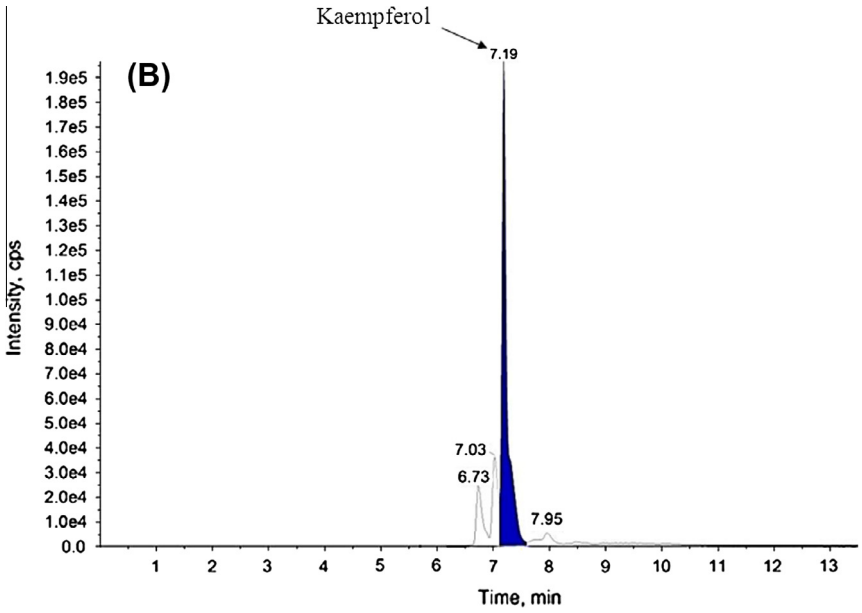

Fig. 1 (*continued*)

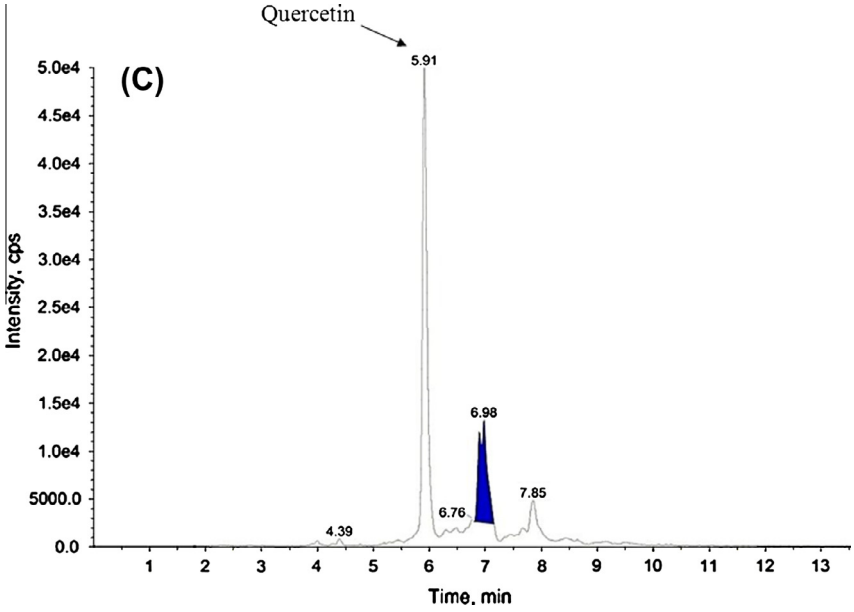

Fig. 1 (*continued*)

(300 mg/kg/day) or lipanthyl, plasma HDL-C concentrations in HFD-fed hamsters increased to 83.8 and 90.9 %, respectively, of the level in the RCD-fed group (Table 1).

Plasma FFA levels in vehicle-treated HFD-fed hamsters were about 2.1-fold that observed in the RCD-fed group (Table 1). The plasma FFA levels decreased by 35.9% in HFD-fed hamsters treated with EEZZR (300 mg/kg/day) compared to their vehicle-treated counterparts (Table 1). Lipanthyl treatment reduced FFA concentrations in HFD-fed hamsters by 42.0% relative to the level in vehicle-treated HFD-fed hamsters (Table 1).

3.4. Effects of treatments on hepatic steatosis

The hepatic levels of TC and TG were significantly higher in HFD-fed hamsters than in those in the RCD-fed group; TC and TG levels were reduced by 35.4% and 42%, respectively, in HFD-fed hamsters treated with lipanthyl (100 mg/kg/day; Table 1). The hepatic TC level was reduced by 24.1% in HFD-fed hamsters treated with EEZZR (300 mg/kg/day; Table 1). EEZZR treatment (300 mg/kg/day) of HFD-fed hamsters also resulted in a significant reduction (35.7%) in hepatic TG concentrations (Table 1).

Photomicrographs of H&E stained liver samples show that HFD feeding increased hepatic fat deposits, as the majority of hepatocytes in HFD-fed hamster livers were distended by fat (Fig. 2). H&E stained liver samples also demonstrated macrovesicular steatosis in the hepatocytes of HFD-fed hamsters; many single large droplets had displaced the nuclei, and ballooning degeneration was apparent, with conspicuous swelling of the cell and cytoplasmic vacuolation (Fig. 2). The treatment of HFD-fed hamsters with EEZZR or lipanthyl reduced the occurrence of fatty liver deposits

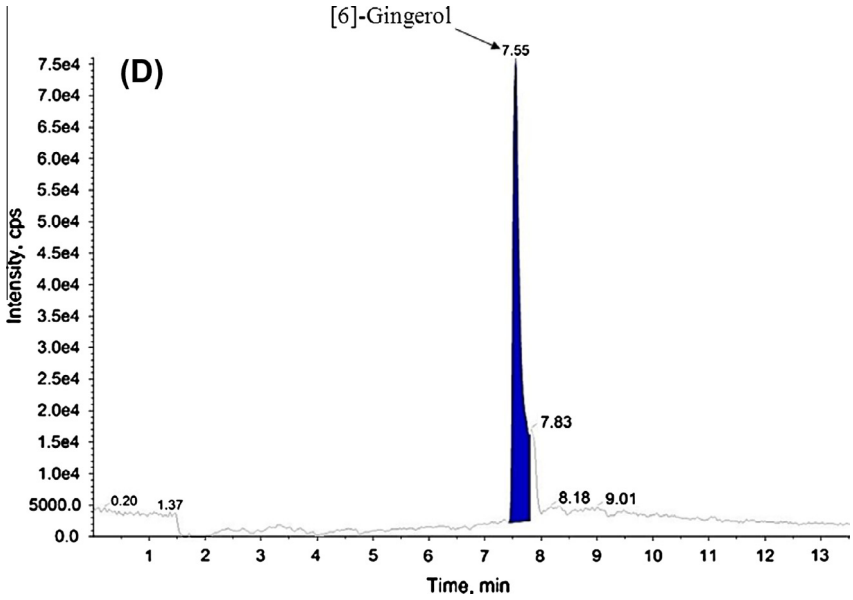

Fig. 1 (*continued*)

Table 1
Summary of metabolic parameters in RCD and HFD-fed hamsters receiving 8-weeks treatments.

	RCD-fed	HFD-fed				
	Vehicle	Vehicle	EEZZR (mg/kg/day)			Lipanthyl (100 mg/kg/day)
			100	200	300	
Body weight (BW) (g)	123.42 ± 8.82[d]	159.52 ± 6.94[b]	153.74 ± 7.82 [b]	149.46 ± 6.11[b]	143.01 ± 7.13[a,c]	138.51 ± 7.82[d]
Food intake (g/day)	9.67 ± 3.93	10.87 ± 3.88	10.63 ± 3.65	10.77 ± 4.56	9.82 ± 4.12	10.83 ± 3.92
Water intake (ml/day)	11.07 ± 4.13	12.47 ± 3.96	12.24 ± 4.21	11.92 ± 3.73	11.44 ± 4.03	11.73 ± 3.26
Liver weight (g/100 g BW)	4.39 ± 0.17[c]	5.11 ± 0.25[a]	4.92 ± 0.18[a]	4.68 ± 0.27	4.61 ± 0.31	4.48 ± 0.23[c]
Plasma glucose (mmol/l)	5.45 ± 0.25[d]	8.69 ± 0.26[b]	7.98 ± 0.21[b]	7.76 ± 0.23[b,c]	7.51 ± 0.25[b,c]	6.62 ± 0.19[a,c]
Plasma insulin (mU/ml)	22.81 ± 0.22[d]	42.93 ± 0.45[b]	39.54 ± 0.37[b,c]	33.88 ± 0.31[b,c]	30.49 ± 0.29[b,c]	28.24 ± 0.32[a,d]
HOMA-IR	5.53 ± 0.19	16.58 ± 0.37[b]	14.02 ± 0.35[b,c]	11.68 ± 0.29[b,c]	10.17 ± 0.28[b,d]	8.31 ± 0.26[a,d]
Plasma TC (mmol/l)	3.90 ± 0.16[d]	5.26 ± 0.19[b]	5.02 ± 0.25[b]	4.58 ± 0.18[b,c]	4.36 ± 0.16[a,d]	4.17 ± 0.18[d]
Plasma TG (mmol/l)	0.42 ± 0.05[d]	1.39 ± 0.09[b]	1.24 ± 0.11[b]	1.06 ± 0.08[b,c]	0.90 ± 0.07[b,d]	0.71 ± 0.09[a,d]
Plasma LDL (mmol/l)	2.75 ± 0.17[d]	4.26 ± 0.21[b]	3.98 ± 0.25[b]	3.48 ± 0.16[b,c]	3.55 ± 0.23[a,d]	3.08 ± 0.18[a,d]
Plasma HDL (mmol/l)	1.11 ± 0.09	0.79 ± 0.11[a]	0.87 ± 0.08[a]	0.89 ± 0.12	0.93 ± 0.07	1.01 ± 0.10
Plasma FFAs (mmol/l)	0.63 ± 0.13[d]	1.31 ± 0.28[b]	1.08 ± 0.18[b]	0.97 ± 0.23[b,c]	0.84 ± 0.14[a,d]	0.76 ± 0.19[d]
Plasma MCP-1 (pg/ml)	88.07 ± 12.61[d]	128.52 ± 16.43[b]	115.67 ± 14.78[a,c]	109.25 ± 15.6[a,c]	98.12 ± 10.37[c]	90.36 ± 11.59[d]
Plasma TNF-α (pg/ml)	238.46 ± 19.34[d]	349.73 ± 20.27[b]	329.56 ± 21.23[b]	305.92 ± 19.38[b]	284.17 ± 17.41[a,c]	279.32 ± 18.29 [a,c]
Plasma IL-6 (pg/ml)	131.24 ± 14.53	225.29 ± 18.73[b]	202.76 ± 16.86	192.62 ± 17.35[b,c]	173.36 ± 18.59[a,d]	156.98 ± 14.72[d]
Hepatic TC (μmol/g liver)	9.76 ± 0.29[d]	19.05 ± 0.34[b]	17.09 ± 0.38[b,c]	15.37 ± 0.43[b,c]	14.51 ± 0.52[a,c]	12.34 ± 0.49[a,d]
Hepatic TG (μmol/g liver)	8.30 ± 0.35[d]	16.45 ± 0.54[b]	15.29 ± 0.51[b]	12.93 ± 0.42[b,c]	10.67 ± 0.49[a,c]	9.61 ± 0.44[a,c]

Zerumbone or lipanthyl was dissolved in distilled water for oral administration at the desired doses in a volume of 1.5 ml/kg once a day into HFD-fed hamsters. The vehicle (distilled water) used to dissolve the tested medications was given at the same volume. Values (mean ± SD) were obtained from each group of 8 animals in each group after 8 weeks of the experimental period.

[a] $p < 0.05$ compared to the values of vehicle-treated RCD-fed hamsters in each group, respectively.
[b] $p < 0.01$ compared to the values of vehicle-treated RCD-fed hamsters in each group, respectively.
[c] $p < 0.05$ compared to the values of vehicle-treated HFD-fed hamsters in each group, respectively.
[d] $p < 0.01$ compared to the values of vehicle-treated HFD-fed hamsters in each group, respectively.

and macrovesicular steatosis compared to that of vehicle-treated counterparts (Fig. 2).

Livers from RCD-fed hamsters did not show any significant macrophage (F4/80-positive cells) infiltration (Fig. 3). In contrast, HFD-fed hamsters demonstrated prominent macrophage infiltration of the liver (Fig. 3). Treatment of HFD-fed hamsters with EEZZR (300 mg/kg/day) or lipanthyl for 8 weeks showed a marked reduction in macrophage influx by 39.5% and 48.5%, respectively, when compared with their vehicle-treated counterparts (Fig. 3).

In addition, the hepatic fibrosis index of α-SMA in HFD-fed hamsters was higher than that of the RCD-fed group (Fig. 4). After treatment with EEZZR (300 mg/kg/day) or lipanthyl for 8 weeks, the hepatic α-SMA levels of HFD-fed hamsters decreased significantly (35.4% and 47.1%, respectively) relative to that of vehicle-treated HFD-fed hamsters (Fig. 4).

3.5. Effects of treatments on inflammatory cytokines in hamsters

In HFD-fed hamsters, the plasma levels of MCP-1, TNF-α, and IL-6 were significantly higher (1.4-, 1.5-, and 1.7-fold, respectively) than those of the RCD-fed group (Table 1). Administration of lipanthyl to HFD-fed hamsters for 8 weeks significantly down-regulated the plasma levels of MCP-1, TNF-α, and IL-6 to 70.3, 79.9, and 69.3%, respectively, of those in vehicle-treated counterparts (Table 1). EEZZR (300 mg/kg/day) treatment reversed the HFD-induced increase of plasma levels of MCP-1, TNF-α, and IL-6 to

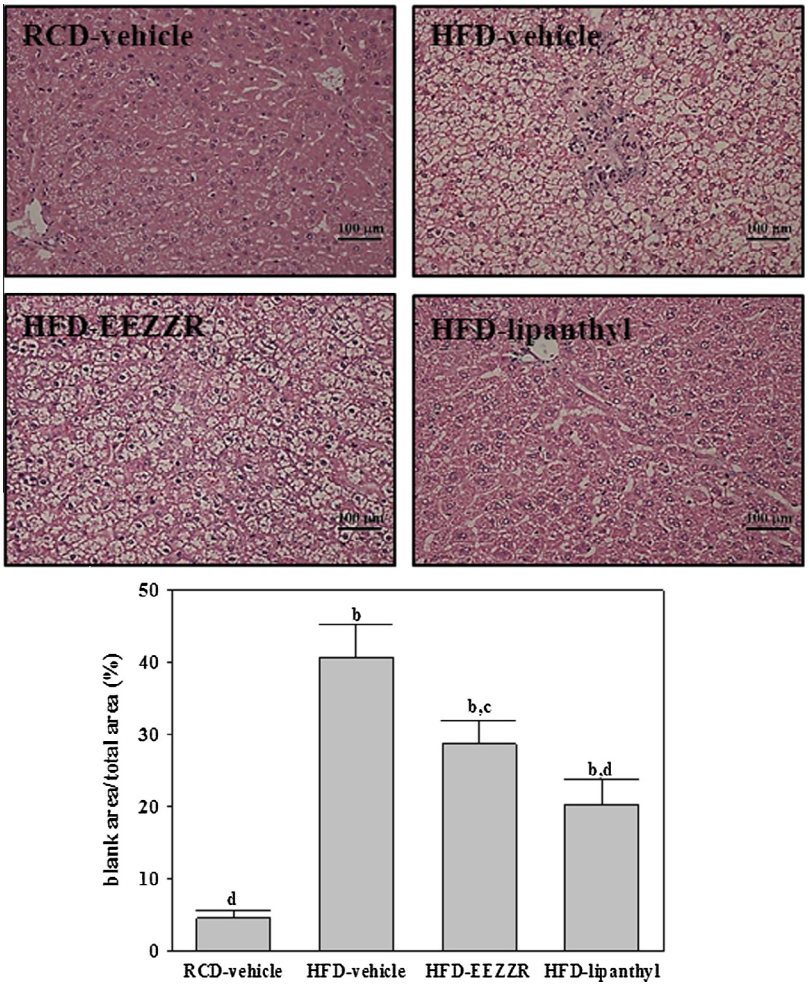

Fig. 2. Representative images of H&E stained livers from RCD- or HFD-fed hamsters receiving 8-weeks of treatment. Photomicrographs are of tissues isolated from vehicle-treated RCD-fed hamsters (RCD-vehicle), vehicle-treated HFD-fed hamsters (HFD-vehicle), EEZZR (300 mg/kg/day)-treated HFD-fed hamsters (HFD-EEZZR), or lipanthyl (100 mg/kg/day)-treated HFD-fed hamsters (HFD-lipanthyl). Quantification of hepatic lipid droplet accumulation is presented as the percentage of the blank area (lipid droplets) relative to the whole area of the photomicrograph. Values (mean ± SD) were obtained from 5 animals in each group. $^{b}p < 0.01$ compared to vehicle-treated RCD-fed hamsters. $^{c}p < 0.05$ and $^{d}p < 0.01$ compared to vehicle-treated HFD-fed hamsters in each group, respectively.

76.3, 81.3 and 76.9%, respectively, of those observed in vehicle-treated counterparts (Table 1).

3.6. Effects of treatment on hepatic mRNA expression of SREBP-1c and its lipogenic target genes

HFD feeding markedly increased the hepatic mRNA levels of SREBP-1c in hamsters to 2.3-fold that of the RCD-fed group (Fig. 5A). Hepatic mRNA levels of SREBP-1c were significantly reduced (by 38.3%) in lipanthyl-treated HFD-fed hamsters compared to vehicle-treated counterparts (Fig. 5A). EEZZR (300 mg/kg/day) suppressed the HFD-induced increase in hepatic mRNA levels of SREBP-1c by 27.3% relative to vehicle-treated counterparts (Fig. 5A).

HFD caused a 2.0-fold induction of hepatic ACC1 mRNA, a 2.1-fold induction of hepatic FAS mRNA, and a 1.7-fold induction of hepatic SCD1 mRNA over those of the RCD-fed group (Fig. 5A). The HFD-induced the mRNA levels of ACC1, FAS, and SCD1 in liver were significantly reversed after lipanthyl treatment (decreased by 36.1%, 37.7%, and 28.3%, respectively) compared to those of vehicle-treated counterparts (Fig. 5A). Hepatic mRNA levels of ACC1, FAS, and SCD1 were downregulated by EEZZR (300 mg/kg/day) treatment, with decreases of 21.3%, 21.2%, and 16.2%, respectively, below those observed in vehicle-treated counterparts (Fig. 5A).

3.7. Effects of treatment on hepatic mRNA expression of PPARα and its target genes responsible for fatty acid β-oxidation

The mRNA levels of PPARα in livers of HFD-fed hamsters were decreased to 47.3% of those of the RCD-fed group (Fig. 5B). Administration of lipanthyl or EEZZR (300 mg/kg/day) to HFD-fed hamsters for 8 weeks significantly up-regulated hepatic PPARα mRNA levels to 1.4- and 1.6-fold that of vehicle-treated counterparts, respectively (Fig. 5B).

Hepatic mRNA levels of CPT-1, ACO, and ACOX1 in HFD-fed hamsters were clearly lower than those of the RCD-fed group and were up-regulated by lipanthyl treatment (162.9%, 179.1%, and 157.4% increases, respectively) (Fig. 5B). The hepatic mRNA levels of CPT-1, ACO, and ACOX1 in HFD-fed hamsters receiving EEZZR (300 mg/kg/day) treatment were increased to 144.4%, 151.2%, and 133.3%, respectively, relative to the expression levels in vehicle-treated counterparts (Fig. 5B).

4. Discussion

The HFD-induced animal model of NAFLD has been widely used to study its pathogenesis and evaluate new treatments (Lieber et al., 2004). In our study, HFD-fed hamsters developed hepatic

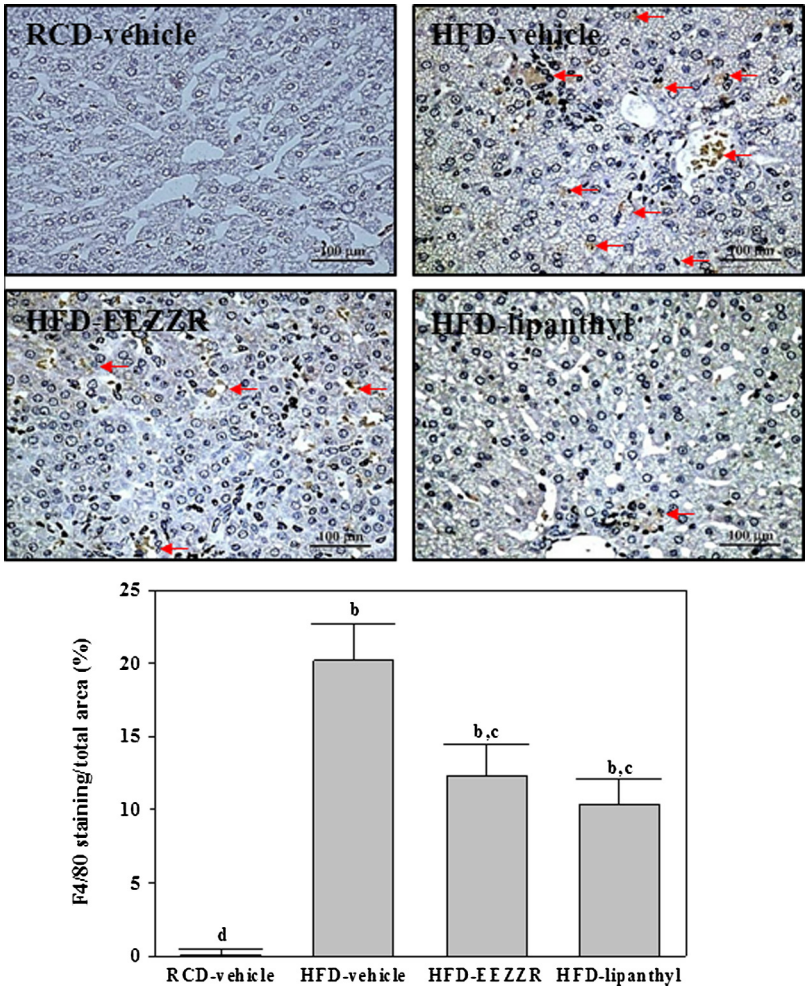

Fig. 3. Representative images of F4/80 staining in livers from RCD- or HFD-fed hamsters receiving 8-weeks of treatment. Photomicrographs are of tissues isolated from vehicle-treated RCD-fed hamsters (RCD-vehicle), vehicle-treated HFD-fed hamsters (HFD-vehicle), EEZZR (300 mg/kg/day)-treated HFD-fed hamsters (HFD-EEZZR), or lipanthyl (100 mg/kg/day)-treated HFD-fed hamsters (HFD-lipanthyl). Arrows indicate inflammatory foci. Quantification of hepatic macrophage accumulation is presented as the percentage of the brown stained area relative to the whole area of the photomicrograph. Values (mean ± SD) were obtained from 5 animals in each group. $^{b}p < 0.01$ compared to vehicle-treated RCD-fed hamsters. $^{c}p < 0.05$ and $^{d}p < 0.01$ compared to the values of vehicle-treated HFD-fed hamsters in each group, respectively.

steatosis, hyperlipidemia, and increased FFA and HOMA-IR values, mimicking almost all of the clinical features of human NAFLD (Lieber et al., 2004). With EEZZR treatment of HFD-fed hamsters, we observed that the increased plasma levels of TG, TC, LDL-C, and FFA were significantly suppressed, whereas the decreased plasma HDL-C levels were clearly elevated . In addition, the relative liver weight of EEZZR treated hamsters was significantly lower than that of HFD-fed hamsters. Morphologically, the livers of HFD-fed hamsters showed large, abundant lipid droplets and clear derangement compared to those of RCD-fed hamsters. However, the livers of HFD-fed hamsters receiving EEZZR had fewer lipid droplets and more normal liver morphology, suggesting that EEZZR had the beneficial effects of preventing lipid accumulation and reversing disrupted liver structure.

As inflammation plays a pivotal role in NAFLD, an important pharmacological objective in treating this disorder is the direct targeting of inflammatory activation (Braunersreuther et al., 2012). EEZZR reduced hepatic macrophage infiltration in HFD-fed hamsters. Our data also demonstrated that treatment with EEZZR decreased plasma concentrations of MCP-1, TNF-α, and IL-6. Expression of α-SMA has been considered one of the dominant features of hepatic stellate cell (HSC) activation and has become an important evaluation index for hepatic fibrosis (Mormone et al., 2011). We observed that the expression of α-SMA was significantly reduced, suggesting that the inhibition of inflammatory factor expression also effectively suppressed HSC activation, blocking the occurrence of hepatic fibrosis at the source. Besides the direct effects of inflammatory cytokines on lipogenesis and fibrogenesis, MCP-1, TNF-α, and IL-6 can induce insulin resistance (Kanda et al., 2006; Li et al., 2013). Importantly, insulin resistance is further associated with the development of steatosis and liver fibrosis (Ibrahim et al., 2013). We observed that the effects of EEZZR treatment were similar to those of lipanthyl on hyperinsulinemia and improved HOMA-IR, although its potency was much less than that of lipanthyl, as higher doses (300 mg/kg/day) of EEZZR than lipanthyl (100 mg/kg/day) were needed. These results further suggest that EEZZR not only suppresses the recruitment of macrophages but also inhibits the release of inflammatory cytokines from hepatic macrophages, preventing hepatic steatosis, fibrosis, and insulin resistance.

To explore the possible mechanisms whereby EEZZR decreases hepatic lipid accumulation, we investigated the expression levels of several genes related to lipid metabolism, including lipogenesis and β-oxidation. SREBP-1c has been shown to regulate the transcription of genes in the lipogenic pathway (Osborne, 2000) including ACC1, FAS, and SCD1. ACC1 mediates the initial step of fatty acid synthesis. Liver-specific ACC1 knockout mice show decreased hepatic triglyceride accumulation, suggesting that ACC1 plays a

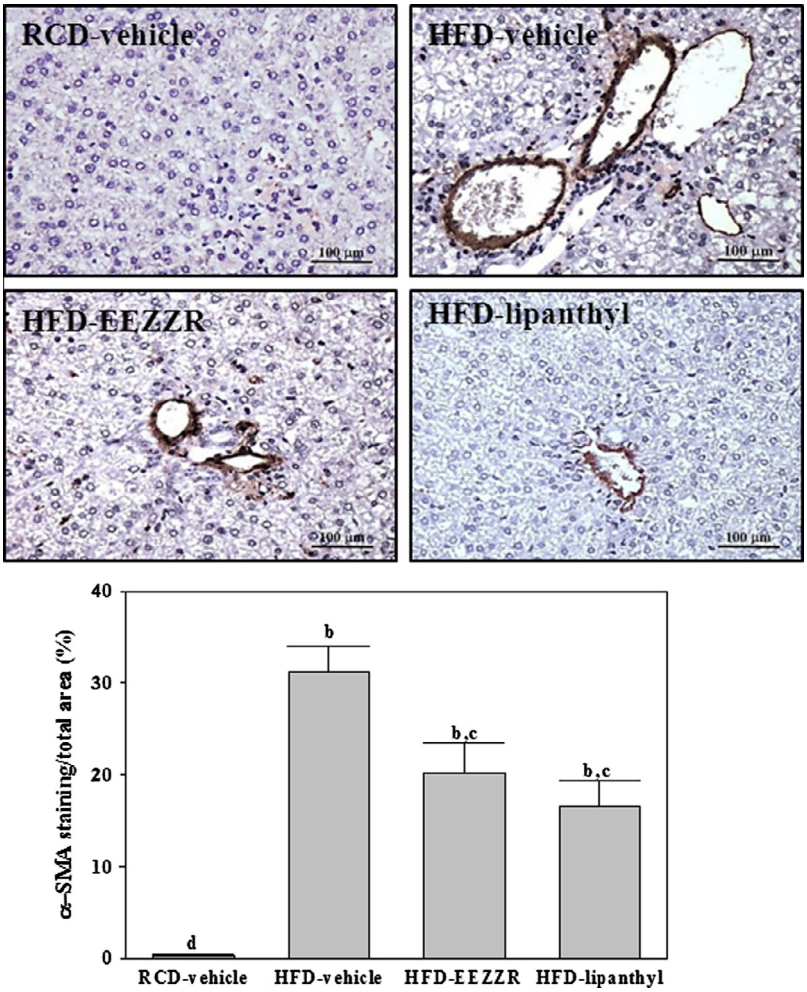

Fig. 4. Representative images of α-SMA staining in livers from RCD- or HFD-fed hamsters receiving 8 weeks of treatment. Photomicrographs are of tissues isolated from vehicle-treated RCD-fed hamsters (RCD-vehicle), vehicle-treated HFD-fed hamsters (HFD-vehicle), EEZZR (300 mg/kg/day)-treated HFD-fed hamsters (HFD-EEZZR), or lipanthyl (100 mg/kg/day)-treated HFD-fed hamsters (HFD-lipanthyl). Quantification of hepatic α-SMA accumulation is presented as the percentage of the brown stained area relative to the whole area of the photomicrograph. Values (mean ± SD) were obtained from 5 animals in each group. $^{b}p < 0.01$ compared to vehicle-treated RCD-fed hamsters. $^{c}p < 0.05$ and $^{d}p < 0.01$ compared to the values of vehicle-treated HFD-fed hamsters in each group, respectively. (For interpretation of the references to color in this figure legend, the reader is referred to the web version of this article.)

crucial role in the regulation of lipogenesis (Mao et al., 2006). FAS catalyzes the last step in fatty acid biosynthesis and is thus believed to be a major determinant of the maximal hepatic capacity to generate fatty acids by *de novo* lipogenesis (Jensen-Urstad and Semenkovich, 2012). SCD1 catalyzes the rate-limiting step in the production of the monounsaturated fatty acids that are major components of tissue lipids (Dobrzyn and Ntambi, 2005). Hence, suppression of SREBP-1c expression in liver may reduce lipid accumulation via downregulation of SCD1. Low levels of SREBP-1c mRNA in the livers of HFD-fed hamsters receiving EEZZR were accompanied by a concomitant significant reduction in the expression of ACC1, FAS, and SCD1 mRNA. EEZZR is thus likely to have a direct inhibitory effect on SREBP-1c expression, which in turn decreases transcription of its target lipogenic genes, thereby reducing enzyme activity and resulting in a low rate of lipid synthesis. These results suggest that EEZZR can ameliorate HFD-induced hepatic steatosis via downregulation of lipid synthesis.

β-Oxidation of lipids in the liver is regulated by multiple transcription factors. The HFD-induced accumulation of hepatic lipids might be the result of a decrease in the β-oxidation of fatty acids (Rector et al., 2008). PPARα is thought to be the principal regulator of the fatty acid oxidation (Reddy and Hashimoto, 2001). Reduced hepatic PPARα expression is indicative of impaired β-oxidation of fatty acids, which may further influence the imbalance of lipid metabolism toward lipid accumulation in the case of induced lipogenic transcription. ACOX1 is the first and rate-limiting enzyme in the PPARα-regulated and peroxisome proliferator-inducible β-oxidation of fatty acids (Huang et al., 2012). To explore whether the effect of EEZZR on the attenuation of HFD-induced hepatic steatosis was related to the PPARα-mediated pathway, mRNA expression of PPARα and its target genes responsible for β-oxidation of fatty acids was measured. EEZZR markedly increased the HFD-induced low expression of hepatic PPARα mRNA. Similarly, EEZZR treatment up-regulated the PPARα-mediated transcription of ACOX1, CPT-1, and ACO mRNA in the liver of HFD-fed hamsters. CPT-1 is the rate-limiting enzyme in the β-oxidation of fatty acids, and its activity is used as a measure of mitochondrial oxidation activity (Bartlett and Eaton, 2004). ACO was chosen as marker because it is a control point in peroxisomal β-oxidation (Poirier et al., 2006). The similar trend in expression among these genes suggests that EEZZR enhanced β-oxidation in liver via the pathway involving PPARα-mediated gene transcription. Taken together, these results suggest that the effect of EEZZR on hepatic steatosis may be partly due to increased expression of the genes involved in the β-oxidation of fatty acids through PPARα activation.

A considerable amount of flavonoids, including kaempferol, quercetin, and [6]-gingerol, are present in EEZZR. These compounds have been shown to exert an effect on lipid catabolism,

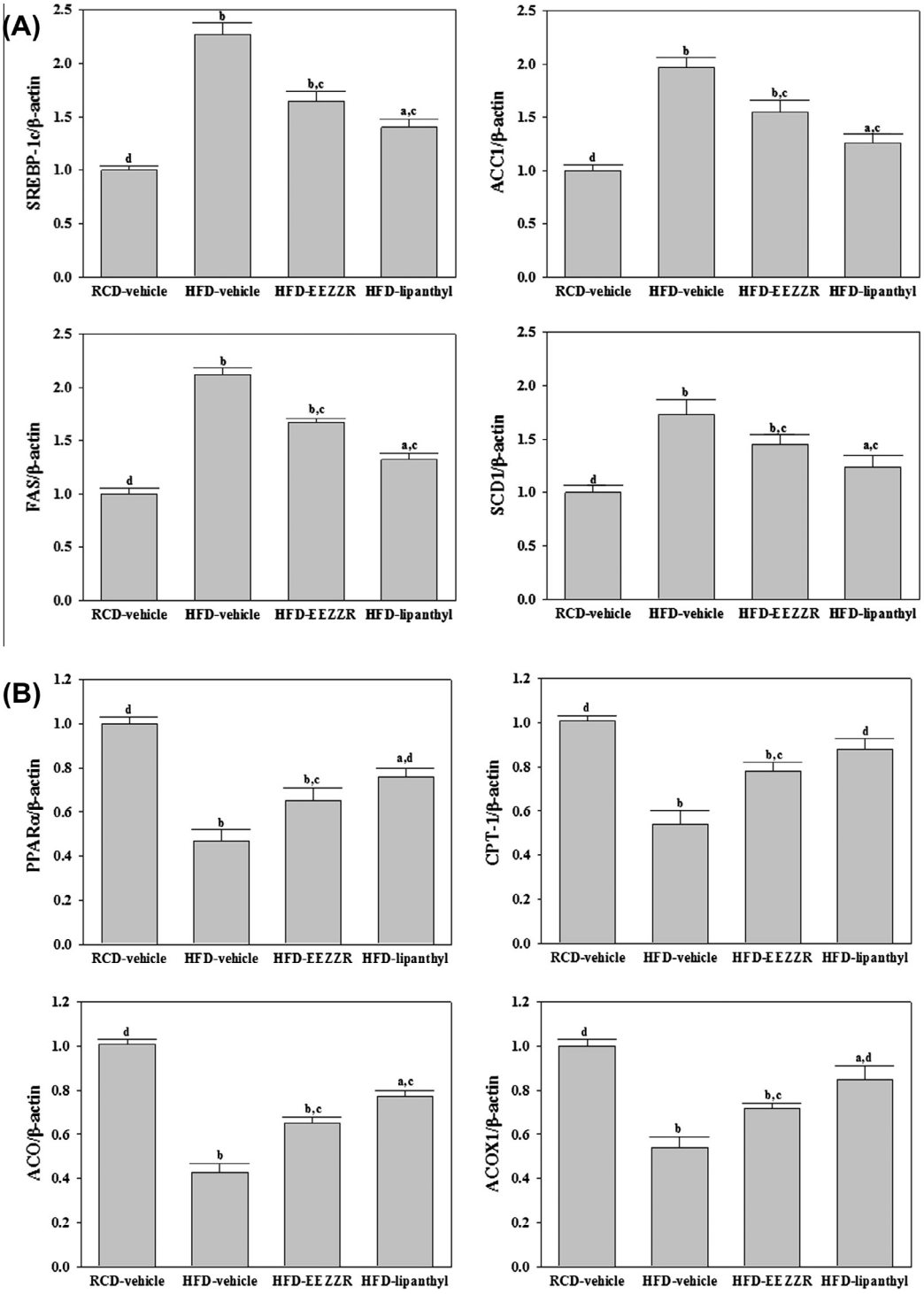

Fig. 5. The hepatic mRNA levels of SREBP-1c and its lipogenic target genes (A), PPARα and its target genes responsible for fatty acid β-oxidation (B) in RCD- or HFD-fed hamsters receiving 8-weeks of treatment. Livers were isolated from vehicle-treated RCD-fed hamsters (RCD-vehicle), vehicle-treated HFD-fed hamsters (HFD-vehicle), EEZZR (300 mg/kg/day)-treated HFD-fed hamsters (HFD-EEZZR), or lipanthyl (100 mg/kg/day)-treated HFD-fed hamsters (HFD-lipanthyl). mRNA expression of the target genes was measured by RT-PCR and normalized to an internal control (β-actin). Similar results were obtained from an additional 4 replications. Data are expressed as the mean with SD ($n = 5$ per group) in each column. $^{a}p < 0.05$ and $^{b}p < 0$ .01 compared to vehicle-treated RCD-fed hamsters in each group, respectively. $^{c}p < 0.05$ and $^{d}p < 0.01$ compared to vehicle-treated HFD-fed hamsters in each group, respectively.

insulin receptor function, and PPAR activation (Crozier et al., 2009). ZZR has been reported to contain cyclic sesquiterpene zerumbone as the major component and shows strong anti-oxidative and anti-inflammatory activities (Yob et al., 2011). We will attempt to identify the specific components of EEZZR responsible for its protective effects against hepatic accumulation and ameliorative hepatic insulin resistance in future studies.

Using a metabolism coefficient of 6.25 to convert the effective daily oral dose of EEZZR for hamsters (300 mg/kg) into a clinical dose, assuming an average adult body weight of 60 kg (Hodge et al., 1967), we estimated a daily oral dose of EEZZR for humans to be approximately 2.8 g. Due to different fat/lipid metabolism in humans and rodents, the results come from animal studies cannot generalize to human. The placebo controlled human studies are

required to find the usability of EEZZR in human NAFLD indications. Also safety testing should be taken with the chronic consumption of large doses of the extract, especially in pregnant women, children, old people, people with kidney diseases.

In conclusion, our results show that EEZZR has the beneficial effects of inhibiting fat accumulation in liver, improving insulin resistance, inhibiting inflammation, and repressing hepatic lipogenesis. All these effects are associated with the inhibition of SREBP-1c and induction of PPARα, suggesting a potential use for EEZZR in treating fatty liver diseases.

5. Conflict of Interest

The authors declare that there are no conflicts of interest.

Acknowledgement

The present study was supported by a Grant from the National Science Council (NSC 102-2324-B-127-001-CC2) of Taiwan, the Republic of China.

References

Bartlett, K., Eaton, S., 2004. Mitochondrial Beta-oxidation. Eur. J. Biochem. 271, 462–469.

Beaton, M.D., 2012. Current treatment options for nonalcoholic fatty liver disease and nonalcoholic steatohepatitis. Can. J. Gastroenterol. 26, 353–357.

Bhathena, J., Kulamarva, A., Martoni, C., Urbanska, A.M., Malhotra, M., Paul, A., Prakash, S., 2011. Diet-induced metabolic hamster model of nonalcoholic fatty liver disease. Diabetes Metab. Syndr. Obes. 4, 195–203.

Braunersreuther, V., Viviani, G.L., Mach, F., Montecucco, F., 2012. Role of cytokines and chemokines in non-alcoholic fatty liver disease. World J. Gastroenterol. 18, 727–735.

Chan, S.M., Sun, R.Q., Zeng, X.Y., Choong, Z.H., Wang, H., Watt, M.J., Ye, J.M., 2013. Activation of PPARα ameliorates hepatic insulin resistance and steatosis in high fructose-fed mice despite increased endoplasmic reticulum stress. Diabetes 62, 2095–2105.

Chang, C.J., Tzeng, T.F., Liou, S.S., Chang, Y.S., Liu, I.M., 2012a. Beneficial impact of *Zingiber zerumbet* on insulin sensitivity in fructose-fed rats. Planta Med. 78, 317–325.

Chang, C.J., Tzeng, T.F., Liou, S.S., Chang, Y.S., Liu, I.M., 2012b. Regulation of lipid disorders by ethanol extracts from *Zingiber zerumbet* in high-fat diet-induced rats. Food Chem. 132, 460–467.

Crozier, A., Jaganath, I.B., Clifford, M.N., 2009. Dietary phenolics: chemistry, bioavailability and effects on health. Nat. Prod. Rep. 26, 1001–1043.

Dobrzyn, A., Ntambi, J.M., 2005. The role of stearoyl-CoA desaturase in the control of metabolism. Prostaglandins Leukot. Essent. Fatty Acids 73, 35–41.

Folch, J., Lees, M., Sloane-Stanley, G.H., 1957. A simple method for the isolation and purification of total lipids from animal tissues. J. Biol. Chem. 226, 497–506.

Hodge, H.C., Downs, W.L., Panner, B.S., Smith, D.W., Maynard, E.A., 1967. Oral toxicity and metabolism of diuron (N-(3,4-dichlorophenyl)-N′, N′-dimethylurea) in rats and dogs. Food Cosmet. Toxicol. 5, 513–531.

Huang, J., Jia, Y., Fu, T., Viswakarma, N., Bai, L., Rao, M.S., Zhu, Y., Borensztajn, J., Reddy, J.K., 2012. Sustained activation of PPARα by endogenous ligands increases hepatic fatty acid oxidation and prevents obesity in ob/ob mice. FASEB J. 26, 628–638.

Ibrahim, M.Y., Abdul, A.B., Ibrahim, T.A., AbdelWahab, S.I., Elhassan, M.M., Mohan, S., 2010. Attenuation of cisplatin-induced nephrotoxicity in rats using zerumbone. Afr. J. Biotechnol. 9, 4434–4441.

Ibrahim, M.A., Kelleni, M., Geddawy, A., 2013. Nonalcoholic fatty liver disease: current and potential therapies. Life Sci. 92, 114–118.

Jensen-Urstad, A.P., Semenkovich, C.F., 2012. Fatty acid synthase and liver triglyceride metabolism: housekeeper or messenger? Biochim. Biophys. Acta 1821, 747–753.

Kanda, H., Tateya, S., Tamori, Y., Kotani, K., Hiasa, K., Kitazawa, R., Kitazawa, S., Miyachi, H., Maeda, S., Egashira, K., Kasuga, M., 2006. MCP-1 contributes to macrophage infiltration into adipose tissue, insulin resistance, and hepatic steatosis in obesity. J. Clin. Invest. 116, 1494–1505.

Kraja, A.T., Province, M.A., Straka, R.J., Ordovas, J.M., Borecki, I.B., Arnett, D.K., 2010. Fenofibrate and metabolic syndrome. Endocr. Metab. Immune Disord. Drug Targets 10, 138–148.

Li, Y., Ding, L., Hassan, W., Abdelkader, D., Shang, J., 2013. Adipokines and hepatic insulin resistance. J. Diabetes. Res. 2013, 170532.

Lieber, C.S., Leo, M.A., Mak, K.M., Xu, Y., Cao, Q., Ren, C., Ponomarenko, A., DeCarli, L.M., 2004. Model of nonalcoholic steatohepatitis. Am. J. Clin. Nutr. 79, 502–509.

Livak, K.J., Schmittgen, T.D., 2001. Analysis of relative gene expression data using real-time quantitative PCR and the 2-ΔΔCT method. Methods 25, 402–408.

Mao, J., DeMayo, F.J., Li, H., Abu-Elheiga, L., Gu, Z., Shaikenov, T.E., Kordari, P., Chirala, S.S., Heird, W.C., Wakil, S.J., 2006. Liver-specific deletion of acetyl-CoA carboxylase 1 reduces hepatic triglyceride accumulation without affecting glucose homeostasis. Proc. Natl. Acad. Sci. USA 103, 8552–8557.

Matthews, D.R., Hosker, J.P., Rudenski, A.S., Naylor, B.A., Treacher, D.F., Turner, R.C., 1985. Homeostasis model assessment: insulin resistance and beta-cell function from fasting plasma glucose and insulin concentrations in man. Diabetologia 28, 412–419.

Mormone, E., George, J., Nieto, N., 2011. Molecular pathogenesis of hepatic fibrosis and current therapeutic approaches. Chem. Biol. Interact. 193, 225–231.

Osborne, T.F., 2000. Sterol regulatory element-binding proteins (SREBPs): key regulators of nutritional homeostasis and insulin action. J. Biol. Chem. 275, 32379–32382.

Paschos, P., Paletas, K., 2009. Non alcoholic fatty liver disease and metabolic syndrome. Hippokratia 13, 9–19.

Poirier, Y., Antonenkov, V.D., Glumoff, T., Hiltunen, J.K., 2006. Peroxisomal beta-oxidation-a metabolic pathway with multiple functions. Biochim. Biophys. Acta 1763, 1413–1426.

Rector, R.S., Payne, R.M., Ibdah, J.A., 2008. Mitochondrial trifunctional protein defects: clinical implications and therapeutic approaches. Adv. Drug Deliv. Rev. 60, 1488–1496.

Reddy, J.K., Hashimoto, T., 2001. Peroxisomal beta-oxidation and peroxisome proliferator activated receptor alpha: an adaptive metabolic system. Annu. Rev. Nutr. 21, 193–230.

Ruslay, S., Abas, F., Shaari, K., Zainal, Z., Maulidiani, Sirat, H., Israf, D.A., Lajis, N.H., 2007. Characterization of the components present in the active fractions of health gingers (Curcuma xanthorrhiza and *Zingiber zerumbet*) by HPLC-DAD-ESIMS. Food Chem. 104, 1183–1191.

Van Heek, M., Compton, D.S., France, C.F., Tedesco, R.P., Fawzi, A.B., Graziano, M.P., Sybertz, E.J., Strader, C.D., Davis Jr., H.R., 1997. Diet-induced obese mice develop peripheral, but not central, resistance to leptin. J. Clin. Invest. 99, 385–390.

Yob, N.J., Jofrry, S.M., Affandi, M.M., Teh, L.K., Salleh, M.Z., Zakaria, Z.A., 2011. *Zingiber zerumbet* (L.) Smith: a review of its ethnomedicinal, chemical, and pharmacological uses. Evid. Complement. Alternat. Med., 543216.